Tunneling spectroscopy of Luttinger-liquid structures far from equilibrium

D. B. Gutman,[1,2] Yuval Gefen,[3] and A. D. Mirlin[1,2,4,5]
[1]*Institut für Theorie der kondensierten Materie, Universität Karlsruhe, 76128 Karlsruhe, Germany*
[2]*DFG Center for Functional Nanostructures, Universität Karlsruhe, 76128 Karlsruhe, Germany*
[3]*Department of Condensed Matter Physics, Weizmann Institute of Science, Rehovot 76100, Israel*
[4]*Institut für Nanotechnologie, Forschungszentrum Karlsruhe, 76021 Karlsruhe, Germany*
[5]*Petersburg Nuclear Physics Institute, 188300 St. Petersburg, Russia*
(Received 19 March 2009; revised manuscript received 26 May 2009; published 8 July 2009)

We develop a theory of tunneling spectroscopy of interacting electrons in a nonequilibrium quantum wire coupled to reservoirs. The problem is modeled as an out-of-equilibrium Luttinger liquid with spatially dependent interaction. The interaction leads to the renormalization of the tunneling density of states, as well as to the redistribution of electrons over energies. Energy relaxation is controlled by plasmon scattering at the boundaries between regions with different interaction strengths and affects the distribution function of electrons in the wire as well as that of electrons emitted from the interacting regions into noninteracting electrodes.

DOI: 10.1103/PhysRevB.80.045106 PACS number(s): 73.23.−b, 73.40.Gk, 73.50.Td

I. INTRODUCTION

One-dimensional (1D) interacting fermionic systems show remarkable physical properties and are promising elements for future nanoelectronics. The electron-electron interaction manifests itself in a particularly dramatic way in 1D systems, inducing a strongly correlated electronic state—Luttinger liquid (LL).[1–4] A paradigmatic experimental realization of quantum wires is carbon nanotubes;[5] for a recent review see Ref. 6. Further realizations encompass semiconductor,[7] metallic,[8] and polymer nanowires,[9] as well as quantum-Hall edges.[10]

There is currently a growing interest in nonequilibrium phenomena on nanoscales. A tunneling spectroscopy (TS) technique for nonequilibrium nanostructures was developed in Ref. 11. Employing a superconducting tunneling electrode allows one to explore not only the tunneling density of states (TDOS) but also the energy distribution function. The energy relaxation found in this way provides information about inelastic scattering in the system. In a very recent experiment[12] this TS method was applied to a carbon nanotube under strongly nonequilibrium conditions.

In this paper, we develop a theory of TS of a LL out of equilibrium. Specifically, we consider a LL conductor connected, via noninteracting leads, to reservoirs with different electrochemical potentials, $\mu_L - \mu_R = eV$, and different temperatures, T_L, T_R (where the indices L, R stand for left and right movers). It is assumed that the coupling to the leads is adiabatic on the scale of the Fermi wavelength so that no backscattering of electrons takes place. We model the leads as noninteracting 1D wires,[13–15] so that the electron-electron interaction is turned on at the vicinity of the points $x = \pm L/2$ (see Fig. 1). This model is quite generic to properly describe the problem at hand, independent of the actual geometry of the leads. Note also that the 1D setup with strongly nonuniform interaction may be experimentally realized by using external screening gates.

It is known that energy relaxation is absent in a uniform clean LL. Within the golden-rule framework, the lack of energy relaxation for forward scattering processes results from 1D kinematic constraints that do not allow to satisfy the energy and momentum conservation laws simultaneously.[16] On a more formal level, the conservation of energies of individual particles in a spatially uniform LL is protected by the integrability of the system, which implies an infinite number of conservation laws.[17] Inclusion of spatial dependence into the model violates these laws and leads to energy relaxation that takes place at the regions where the interaction varies in space.[18]

The fact that inhomogeneous interaction induces energy relaxation of electrons has been pointed out for the first time in Ref. 19 in the context of interacting quantum-Hall edges but a detailed analysis of this effect has been missing until now. On the other hand, one may expect this to be a dominant effect on the electron distribution function in experiments done on modern high-quality quantum wires (such as ultraclean carbon nanotubes[20]) under nonequilibrium conditions. There is thus a clear need in the theory of TS in nonequilibrium LL.

It is worth noting that we assume the absence of backscattering due to impurities in the wire. When present, such impurities strongly affect the electronic properties of a LL wire: they induce diffusive dynamics at sufficiently high temperature T and localization phenomena proliferating with lowering T (Refs. 21–23), as well as inelastic processes.[24,25] We also neglect the nonlinearity of the electron dispersion

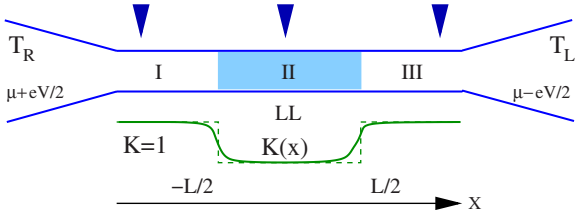

FIG. 1. (Color online) Schematic view of a LL conductor with various positions of tunnel probes. The solid curve in the lower part of the figure shows a spatially dependent LL interaction parameter $K(x)$. The dashed line corresponds to the limit of a sharp variation in $K(x)$ at the boundaries.

whose influence on spectral and kinetic properties of 1D electrons was recently studied in Refs. 16 and 26.

II. FORMALISM

Within the LL model, the electron field is decoupled in a sum of right- and left-moving terms, $\psi(x,t)=\psi_R(x,t)e^{ip_Fx}+\psi_L(x,t)e^{-ip_Fx}$, where p_F is the Fermi momentum. The Hamiltonian of the system reads

$$H = H_0 + H_{\rm int}, \tag{1}$$

$$H_0 = -iv\int dx(\psi_R^\dagger\partial_x\psi_R - \psi_L^\dagger\partial_x\psi_L), \tag{2}$$

$$H_{\rm int} = \frac{1}{2}\int dx g(x)(\psi_R^\dagger\psi_R + \psi_L^\dagger\psi_L)^2, \tag{3}$$

where v is the electron velocity and $g(x)$ is the spatially dependent electron-electron interaction constant.

We will proceed by following the lines of the functional bosonization approach[27] in the nonequilibrium (Keldysh) formulation.[24,28,29] Performing the Hubbard-Stratonovich transformation, one decouples the interaction term via a bosonic field ϕ and gets the action

$$S[\psi,\phi] = i\sum_{\eta=R,L}\psi_\eta^\dagger(\partial_\eta-\phi)\psi_\eta - \frac{1}{2}\phi g^{-1}\phi, \tag{4}$$

where $\partial_{R,L}=\partial_t \pm v\partial_x$ and the fields are defined on the Keldysh time contour. The information about physical observables is contained in Keldysh Green's functions[30] $G^>$ and $G^<$; see, in particular, Appendix A where we express tunneling current in terms of functions $G^\gtrless$ and discuss how its measurement allows one to determine $G^\gtrless$ experimentally. The Green's functions $G^\gtrless$ can be presented in the form

$$G_\eta^\gtrless(x,t;x',t') = \int \mathcal{D}\phi Z[\phi]e^{-(i/2)\phi g^{-1}\phi} \times G_\eta^\gtrless[\phi](x,t;x',t'), \tag{5}$$

where we introduced the Green's function in a given field configuration, $G_\eta^\gtrless[\phi]$, and the sum of vacuum loops, $Z[\phi]$.

In 1D geometry the coupling between the fermionic and bosonic fields can be eliminated by a gauge transformation $\psi_\eta(x,t)\to\psi_\eta(x,t)e^{i\theta_\eta(x,t)}$ if we require

$$i\partial_\eta\theta_\eta = \phi. \tag{6}$$

As a result, $G_\eta^\gtrless[\phi]$ can be cast in the form

$$G_\eta^\gtrless[\phi](x,t;x',t') = G_{\eta,0}^\gtrless(x-x';t-t')e^{-i\eta eV(t-t')/2} \times e^{\Phi_\eta^\gtrless(x,t;x',t')}. \tag{7}$$

Here

$$\Phi_\eta^\gtrless(x,t;x',t') = i\theta_{\pm,\eta}(x,t) - i\theta_{\mp,\eta}(x',t'), \tag{8}$$

$G_{\eta,0}^\gtrless$ is the Green's function of free fermions,

$$G_{\eta,0}^\gtrless(\xi) = \frac{T_\eta}{2v}\frac{1}{\sinh\,\pi T_\eta(\eta\xi_\eta \pm i0)}, \tag{9}$$

the coordinate $\xi_{R/L}=x/v\mp t$ labels the trajectory of a particle, and we use the convention that in formulas η should be understood as $\eta=\pm1$ for right- and left-moving electrons.

It is convenient to perform a rotation in Keldysh space, thus decomposing fields into classical and quantum components, $\phi_1,\phi_2=(\phi_+\pm\phi_-)/\sqrt{2}$, where the indices + and − refer to the fields on two branches of the Keldysh contour. Further, we introduce vector notations by combining ϕ_1 and ϕ_2 in a two-vector $\boldsymbol{\phi}$. To proceed further, we resolve Eq. (6) and express $\boldsymbol{\theta}_\eta$ through $\boldsymbol{\phi}$ as

$$\boldsymbol{\theta}_\eta = \mathcal{G}_{\eta 0}\sigma_1\boldsymbol{\phi}, \tag{10}$$

where $\mathcal{G}_{\eta 0}$ is the Green's function of free bosons,

$$\mathcal{G}_{\eta 0} = \begin{pmatrix} \mathcal{G}_{\eta 0}^K & \mathcal{G}_{\eta 0}^r \\ \mathcal{G}_{\eta 0}^a & 0 \end{pmatrix}. \tag{11}$$

Its retarded and advanced components are given by

$$\mathcal{G}_{\eta 0}^{r,a} = \frac{1}{\omega-\eta vq\pm i0}. \tag{12}$$

The Keldysh component of $\mathcal{G}_{\eta 0}$ is given by $\mathcal{G}_{\eta 0}^K=(\mathcal{G}_{\eta 0}^r-\mathcal{G}_{\eta 0}^a)B_\eta^{(0)}(\omega)$, where $B_\eta^{(0)}(\omega)$ is determined by the temperature T_η of the reservoir from which the electrons moving in direction η emerge,

$$B_\eta^{(0)}(\omega) = \coth\,\omega/2T_\eta. \tag{13}$$

Using Eqs. (8) and (10) and performing a transformation to the coordinate space, we express the exponent $\Phi_\eta^\gtrless[\phi](x,t,x',t')$ through the bosonic field $\phi(y)$,

$$\Phi_\eta^\gtrless[\boldsymbol{\phi}](x,t,x',t') = \int\frac{d\omega}{2\pi}dy\,\boldsymbol{\phi}_{-\omega}^T(y)\boldsymbol{J}_{\eta,\omega}^\gtrless(y;x,t,x',t'). \tag{14}$$

The components of $\boldsymbol{J}$ are found as

$$J_{1,\eta,\omega}^\gtrless(y) = \frac{e^{i\eta(\omega/v)y}}{\sqrt{2}v}\{\theta[\eta(x-y)]e^{-i\omega\xi_\eta}-\theta[\eta(x'-y)]e^{-i\omega\xi_\eta'}\},$$

$$J_{2,\eta,\omega}^\gtrless(y) = -\frac{e^{i\eta(\omega/v)y}}{\sqrt{2}v}(e^{i\omega\xi_\eta}-e^{i\omega\xi_\eta'})B_\eta^{(0)}(\omega) \mp \frac{e^{i\eta(\omega/v)y}}{\sqrt{2}v}\{\theta[\eta(y-x)]e^{-i\omega\xi_\eta}+\theta[\eta(y-x')]e^{-i\omega\xi_\eta'}\}, \tag{15}$$

where $\theta(x)$ is the Heaviside θ function. The vacuum loop factor in Eq. (5) is given by

$$Z[\boldsymbol{\phi}] = \exp\left(-\frac{i}{2}\boldsymbol{\phi}^T\Pi\boldsymbol{\phi}\right), \tag{16}$$

where Π is the polarization operator,

$$\Pi = \begin{pmatrix} 0 & \Pi^a \\ \Pi^r & \Pi^K \end{pmatrix}.$$

It can be decomposed into left- and right-moving parts, $\Pi = \Pi_R + \Pi_L$, with

$$\Pi^r_{R,L} = \frac{1}{2\pi} \frac{q}{v_F q \mp \omega_+}, \quad \Pi^a_{R,L} = \frac{1}{2\pi} \frac{q}{v_F q \mp \omega_-},$$

$$\Pi^K_\eta = (\Pi^r_\eta - \Pi^a_\eta) B^{(0)}_\eta(\omega), \tag{17}$$

where $\omega_\pm = \omega \pm i0$. Performing the averaging over the auxiliary field ϕ, we get

$$G^{\gtrless}_\eta(x,t;x',t') = G^{\gtrless}_{\eta,0}(\xi_\eta - \xi'_\eta) e^{-i\eta eV(t-t')/2} e^{\mathcal{F}^{\gtrless}_\eta}, \tag{18}$$

where the effect of the interaction is represented by the "Debye-Waller factor" $e^{\mathcal{F}^{\gtrless}_\eta}$ with

$$\mathcal{F}^{\gtrless}_\eta(x,t;x',t') = -\frac{i}{2} \int \frac{d\omega}{2\pi} dy_1 dy_2 \times \boldsymbol{J}^{\gtrless,T}_{-\omega,\eta}(y_1) \mathcal{V}_\omega(y_1,y_2) \boldsymbol{J}^{\gtrless}_{\omega,\eta}(y_2). \tag{19}$$

Here

$$\mathcal{V} = (\Pi + g^{-1}\sigma_1)^{-1} \tag{20}$$

is the screened electron-electron interaction potential. Its retarded component is given by

$$\mathcal{V}^r_\omega(y,y') = g(y) \left[\delta(y-y') + \frac{v g(y')}{\pi} \partial_y \partial_{y'} \mathcal{G}^r_\omega(y,y') \right], \tag{21}$$

where the function $\mathcal{G}^r_\omega$ is determined by the following differential equation:

$$[\omega^2 + \partial_y u^2(y) \partial_y] \mathcal{G}^r_\omega(y,y') = \delta(y-y'), \tag{22}$$

which describes the plasmon propagation in a medium with spatially dependent sound velocity $u(x) = v[1 + g(x)/\pi v]^{1/2}$. The Keldysh component of the interaction propagator is obtained as

$$\mathcal{V}^K_\omega(y_1,y_2) = -\frac{i\omega}{2\pi v^2} \sum_{\eta=\pm} B_\eta(\omega) I^\eta_\omega(y_1) I^\eta_{-\omega}(y_2), \tag{23}$$

where

$$I^\eta_\omega(y) = \int dy' e^{i\eta(\omega/v)y'} \mathcal{V}^r_\omega(y,y'). \tag{24}$$

At equilibrium, $B_R(\omega) = B_L(\omega) \equiv B(\omega)$, this reduces to

$$\mathcal{V}^K_\omega = [\mathcal{V}^r_\omega - \mathcal{V}^a_\omega] B(\omega), \tag{25}$$

in agreement with the fluctuation-dissipation theorem.

III. SHARP BOUNDARIES

So far we made no restriction on the way the interaction changes in space. Let us consider first the case when the interaction turns on and off sharply on the scale set by the temperatures, $l_T \sim v/\max\{T_L, T_R\}$. This limit can be modeled via a stepwise interaction as represented by the dashed line in Fig. 1. Equation (22) for $\mathcal{G}^r_\omega$ can be then straightforwardly solved by using the fact that the velocity u is constant in each of three regions and employing the proper boundary conditions [continuity of $\mathcal{G}^r_\omega(y,y')$ and of $u^2(y)\partial_y \mathcal{G}^r_\omega(y,y')$] at $y = \pm L/2$.

In the TS context, we are interested in the Green's functions $G^{\gtrless}$ with coinciding spatial arguments, $x = x'$. Assuming x to be in the interacting part of the wire (and not too close to the boundaries) and setting $t' = 0$, we find

$$\mathcal{F}^{\gtrless}_R = -\gamma \int_0^\infty \frac{d\omega}{\omega} \left[\frac{(1-K)^2 B^{(0)}_R(\omega) + (1+K)^2 B^{(0)}_L(\omega)}{2(1+K^2)} \times (1 - \cos\omega t) \pm i \sin\omega t \right], \tag{26}$$

where

$$K = v/u \equiv (1 + g/\pi v)^{-1/2} \tag{27}$$

is the conventional dimensionless parameter characterizing the interaction strength in a LL and

$$\gamma = \frac{(K-1)^2}{2K}. \tag{28}$$

The integral in Eq. (26) and in analogous formulas below is logarithmically divergent at large frequencies and requires an ultraviolet regularization. Specifically, these integrals are understood as regularized by a factor $e^{-\omega/\Lambda}$, where Λ is an ultraviolet cutoff. Deriving Eq. (26), we have neglected terms of the form $e^{in\omega L/u}$ (with nonzero integer n) that arise due to the Fabry-Pérot-type interference of plasmon modes reflected at the boundaries. Keeping these terms would lead to an additional oscillatory structure in energy[31] with the scale $\pi u/L$. Since we are interested in TS of long wires, we assume that this scale is much less than $\max\{T_R, T_L\}$, so that oscillations are suppressed.

Substituting Eq. (26) into Eq. (18), we finally get the Green's functions,

$$G^{\gtrless}_R(t) = (2\pi i v)^\gamma [G^{\gtrless}_{R,0}(t)]^{1+\alpha} [G^{\gtrless}_{L,0}(t)]^\beta e^{-i\eta eVt/2}, \tag{29}$$

where

$$\alpha = \frac{(K-1)^4}{4K(1+K^2)}, \quad \beta = \frac{(K^2-1)^2}{4K(1+K^2)}. \tag{30}$$

The Green's functions [Eq. (29)] can be determined experimentally from TS measurements[12] (see Appendix A). Their difference determines the TDOS $\nu(\epsilon)$,

$$G^>_\eta(\epsilon,x,x) - G^<_\eta(\epsilon,x,x) = -2\pi i \nu_\eta(\epsilon), \tag{31}$$

while each of them separately (or their sum) also contains information about the distribution function, as discussed below. The results for the TDOS have been found in Ref. 29.

Next we consider the noninteracting parts of the wire and discuss, e.g., the right-moving electrons. In region I (see Fig. 1), $x, x' < -L/2$, we find from Eqs. (19) and (15) that $\mathcal{F}^{\gtrless}_R = 0$, so that the Green's functions of the right movers are not

modified by interaction. Physically this is quite transparent: the right-moving electrons in this part of the system are just coming from the reservoir and are not yet "aware" of the interaction with the left movers.

The situation is distinctly different in region III, $x,x' > L/2$. Assuming $x=x'$, we find

$$\mathcal{F}_R^{\gtrless} = \int_0^\infty \frac{d\omega}{\omega} \frac{(1-K)^2}{1+K^2}(1-\cos\omega t)[B_R^{(0)}(\omega) - B_L^{(0)}(\omega)]. \tag{32}$$

Substituting Eq. (32) into Eq. (18), one gets

$$G_R^{\gtrless}(t) = [G_{R,0}^{\gtrless}(t)]^{\mathcal{T}}[G_{L,0}^{\gtrless}(t)]^{\mathcal{R}} e^{-i\eta eVt/2}, \tag{33}$$

where

$$\mathcal{T} = \frac{2K}{1+K^2}, \quad \mathcal{R} = \frac{(1-K)^2}{1+K^2}. \tag{34}$$

Since $\mathcal{F}_R^{\gtrless}$ in Eq. (32) is real, the TDOS is not affected by the interaction, $\nu_R(\epsilon)=\nu_0 \equiv 1/2\pi v$, as expected. The modification of the functions $G_R^{\gtrless}$ as compared to that of incoming electrons, $G_{R,0}^{\gtrless}$, implies therefore the change in the distribution function $n_R(\epsilon)$ of right movers. Indeed, for noninteracting particles $G_R^{<}=2\pi i \nu_0 n_R(\epsilon)$ and $G_R^{>}=-2\pi i \nu_0[1-n_R(\epsilon)]$. We thus see that the electrons ejected from the interacting part of the wire into the lead are affected by the interaction: their distribution function has changed.

The left-moving electrons can be analyzed in the same way; the corresponding results are obtained by replacing $R \leftrightarrow L, V \leftrightarrow -V$ in Eqs. (29) and (33). Clearly, the roles of regions I and III are interchanged in this case. It is also worth mentioning that in the noninteracting parts of the wire the Green's functions are both Galilean and translationally invariant, depending on coordinates and times via $\xi_\eta - \xi'_\eta$ only.

IV. ARBITRARY BOUNDARIES

We turn now to generalization of these results for the case of an arbitrary shape of $g(x)$ in the contact region between the interacting part of the wire and the noninteracting leads. The contact regions are in general characterized by some reflection coefficients $r_i(\omega)$ for the plasmon amplitude, yielding reflection coefficients $\mathcal{R}_i=|r_i|^2$ for the plasmon intensity ($i=1,2$ for the left and right contacts, respectively). The corresponding transmission coefficients are $\mathcal{T}_i=1-\mathcal{R}_i$. It is instructive in this context to compare our present approach with that developed in Ref. 29, where we analyzed the tunneling density of states and focused on the case of smooth variation in $g(x)$ in the contact regions. As we are going to show, the method in Ref. 29 can be generalized to the case of arbitrary contacts (this was briefly discussed at the end in Ref. 29) and is also useful for the analysis of the electron distribution function. Within that approach, the propagator of bosons is calculated in momentum space (rather than in real space as in the above calculation). The Keldysh component of the propagator is then characterized by distribution functions $B_\eta^{(0)}(\omega)$ and $B_\eta(\omega)$ associated with poles at $q=\eta\omega/v$ and $q=\eta\omega/u$ and describing "ghosts" (free electron-hole pairs) and plasmons, respectively.[32] While the distribution function of ghosts is simply determined by that of incoming electrons, the plasmons experience in general reflection at the boundaries. We have for the left boundary (see Fig. 2)

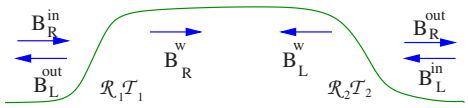

FIG. 2. (Color online) Distribution functions of plasmons B_η in different parts of the wire. The distributions of incoming plasmons are determined by respective leads, $B_\eta^{\rm in}=B_\eta^{(0)}$.

$$B_R^{\rm w} = \mathcal{T}_1 B_R^{(0)} + \mathcal{R}_1 B_L^{\rm w}, \quad B_L^{\rm out} = \mathcal{R}_1 B_R^{(0)} + \mathcal{T}_1 B_L^{\rm w} \tag{35}$$

and similarly at the right boundary. Here we have introduced the notation $B_\eta^{\rm w}$ for plasmon distributions in the interacting region of the wire and $B_\eta^{\rm out}$ for outgoing channels. Solving these equations, we find the plasmon distribution functions of right movers in the interacting part of the wire, as well as in the outgoing channel (in the right lead),

$$B_R^{\rm w} = \frac{\mathcal{T}_1}{1-\mathcal{R}_1\mathcal{R}_2} B_R^{(0)} + \frac{\mathcal{T}_2\mathcal{R}_1}{1-\mathcal{R}_1\mathcal{R}_2} B_L^{(0)}, \tag{36}$$

$$B_R^{\rm out} = \frac{\mathcal{T}_1\mathcal{T}_2}{1-\mathcal{R}_1\mathcal{R}_2} B_R^{(0)} + \frac{\mathcal{T}_1+\mathcal{T}_2-2\mathcal{T}_1\mathcal{T}_2}{1-\mathcal{R}_1\mathcal{R}_2} B_L^{(0)}. \tag{37}$$

The corresponding results for left movers are obtained by exchanging the indices $R \leftrightarrow L$ and $1 \leftrightarrow 2$.

The method in Ref. 29 allows us to express the exponents $\mathcal{F}_\eta^{\gtrless}$ in terms of these distribution functions. For the interacting part of the wire, we get

$$\mathcal{F}_R^{\gtrless} = -\int_0^\infty \frac{d\omega}{\omega}\{(B_R^{\rm w} - B_R^{(0)})(1-\cos\omega t) + \gamma[(B_R^{\rm w} + B_L^{\rm w})(1-\cos\omega t) \pm i\sin\omega t]\}. \tag{38}$$

The result for the tunneling into the noninteracting region III of Fig. 1 can be obtained from Eq. (38) by using the distribution functions $B_\eta^{\rm out}$ corresponding to this region and replacing the interaction constant γ by zero,

$$\mathcal{F}_R^{\gtrless} \equiv \mathcal{F}_R = -\int_0^\infty \frac{d\omega}{\omega}(B_R^{\rm out} - B_R^{(0)})(1-\cos\omega t) = \int_0^\infty \frac{d\omega}{\omega}\mathcal{R}(1-\cos\omega t)[B_R^{(0)}(\omega) - B_L^{(0)}(\omega)], \tag{39}$$

where $\mathcal{R}$ is the total reflection coefficient on a double-step structure, $\mathcal{R}=1-\mathcal{T}_1\mathcal{T}_2/(1-\mathcal{R}_1\mathcal{R}_2)$.

For the case of sharp boundaries the reflection and transmission coefficients are given by the Fresnel law, $\mathcal{R}_{1,2}=(1-K)^2/(1+K)^2$ and $\mathcal{T}_{1,2}=4K/(1+K)^2$, so that Eqs. (38) and (39) reduce to earlier results (26) and (32). The total reflection and transmission coefficients $\mathcal{R}$ and $\mathcal{T}$ take in this case value (34) (which explains the notations introduced there). Clearly, general formulas (38) and (39) can also be obtained in the framework of a real-space calculation that was presented above for sharp boundaries. To do this, one

has to modify the boundary conditions for the Green's function in $\mathcal{G}^r_\omega$ in Eq. (22) by including the appropriate reflection and transmission amplitudes $r_i(\omega)$ and $t_i(\omega)$ at two boundaries and then proceeding in the same way as in course of the derivation of Eqs. (26) and (32). The two methods (real space and k space) are thus in full agreement with each other.

The formal results obtained thus far can be implemented to obtain physical observables. Consider first the noninteracting part of the setup, region III of Fig. 1. The effect of the interaction there amounts to modification of the distribution function of outgoing particles (right movers), which has (in time domain) the form

$$n_R(t) = n_{R,0}(t)e^{\mathcal{F}_R(t)}, \tag{40}$$

where $\mathcal{F}_R$ is given by Eq. (39). This yields

$$n_R(t) = \frac{i}{2}e^{-ieVt/2}\left(\frac{T_R}{\sinh \pi T_R t + i0}\right)^{\mathcal{T}}\left(\frac{T_L}{\sinh \pi T_L t + i0}\right)^{\mathcal{R}}. \tag{41}$$

The way in which the electron distribution function is modified depends on the kinetics of the plasmons inside the interacting region. For adiabatic switching of interaction, there is essentially no plasmon scattering. Therefore, the total reflection coefficient $\mathcal{R}$ and, consequently, the exponent $\mathcal{F}_R$ in region III vanish. In this case the fermions retain their distribution function: the right movers going out into the right lead have the same distribution as the right movers injected into the interacting region from the left lead. (The same applies to the left movers, of course.) Let us now discuss the opposite limit of strong reflection, $\mathcal{R}\to 1$. For a structure with a sharp boundary, this is the case provided the interaction is strong, $K\to 0$. Alternatively, this limit may be realized if the boundary regions are sufficiently extended and characterized by random $K(x)$ such that plasmons with relevant frequencies are localized. Regardless of the cause, in the limit $\mathcal{R}\to 1$ the left- and right-moving electrons exchange their distribution functions except for keeping their total flux (i.e., the chemical potential).

Next, we consider the interacting part of the wire. Analyzing result (38), we see that two terms in square brackets have distinctly different physical origins. The second term, which is proportional to the local strength of the interaction γ at the measurement point, is responsible for creation of the zero-bias anomaly (ZBA) as well as for its dephasing smearing, with the nonequilibrium dephasing rate[29]

$$\tau_\phi^{-1} = \pi\gamma\left[\frac{(1-\mathcal{R}_1)(1+\mathcal{R}_2)}{1-\mathcal{R}_1\mathcal{R}_2}T_R + \frac{(1+\mathcal{R}_1)(1-\mathcal{R}_2)}{1-\mathcal{R}_1\mathcal{R}_2}T_L\right]. \tag{42}$$

On the other hand, the first term in the integrand of Eq. (38), which is governed by the difference between the incoming and local distribution of plasmons, is fully analogous to the expression for $\mathcal{F}^{\gtrless}$ in the noninteracting region [Eq. (39)] and describes the modification of the distribution function inside the wire,

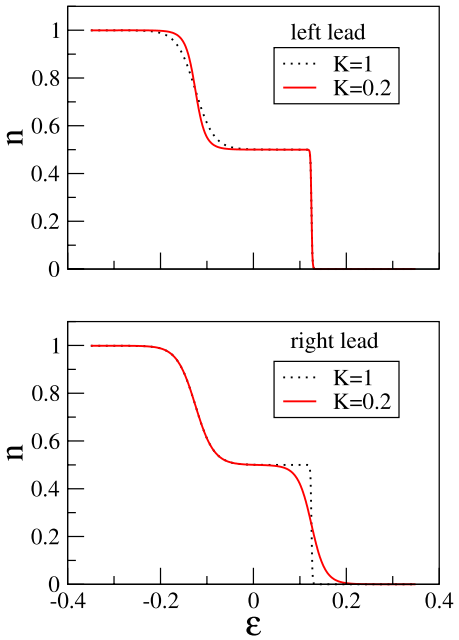

FIG. 3. (Color online) Total distribution functions of electrons in the left and right leads for the LL interaction parameters $K=1$ (no interaction) and $K=0.2$ (with sharp boundaries). Temperatures of the leads are $T_L=0.2$ and $T_R=0.001$; the bias voltage is $eV=0.25$.

$$n_\eta(t) = n_{\eta,0}(t)\exp\left\{-\int_0^\infty \frac{d\omega}{\omega}[B^{\mathrm{w}}_\eta(\omega) - B^{(0)}_\eta(\omega)](1-\cos\omega t)\right\}$$
$$= \frac{i}{2\pi t + i0}\frac{1}{}\exp\left\{-\int_0^\infty \frac{d\omega}{\omega}[B^{\mathrm{w}}_\eta(\omega) - 1](1-\cos\omega t)\right\}. \tag{43}$$

As is clear from Eq. (43), the ghost term with $B^{(0)}_\eta$ essentially serves to cancel the bare distribution function $n_{\eta,0}$, so that the distribution function $n(t)$ is determined only by the plasmonic distribution $B^{\mathrm{w}}_\eta(\omega)$ in the wire. This is, in fact, a manifestation of a general relation between the functional and full bosonization approaches, as will be discussed in detail elsewhere.[33]

Fourier transformation of our results into the energy representation can be done numerically (for analytic calculation at equilibrium, see Appendix B); representative results are shown in Figs. 3 and 4. In Fig. 3 we present distribution functions for noninteracting parts of the wire. Temperatures are set to $T_L=0.2$ and $T_R=0.001$ (in arbitrary units), the applied voltage is $eV=0.25$, and a sharp variation in the interaction at the boundaries (as in Sec. III) is assumed. The distribution function of free fermions ($K=1$), plotted by a dashed line, is the same on both ends of the wire. For interacting electrons [we choose the interaction parameter to be $K=0.2$, which is in the range of characteristic values reported for carbon nanotubes (see, e.g., Ref. 5)] the distribution functions in two leads are different. In particular, the distribution function in the left lead (region I in Fig. 1) has a sharp edge at the energy $\epsilon=\mu+eV/2$, which corresponds to cold right-moving electrons. In the right lead (region III), this edge is broadened due to interaction with hot left-moving electrons.

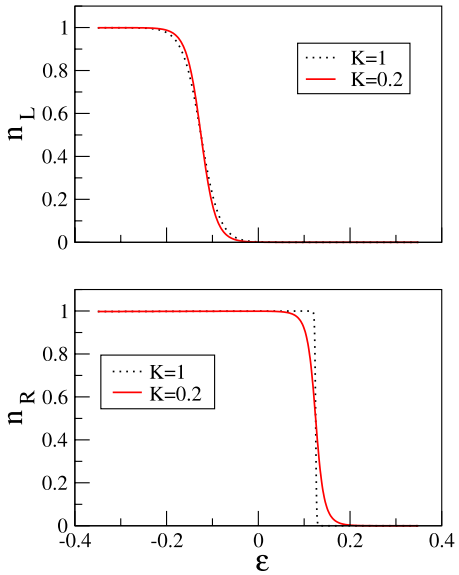

FIG. 4. (Color online) Distribution functions of left and right movers [Eq. (43)] in the interacting part of the wire. All parameters are the same as in Fig. 3.

The situation is opposite for left-moving particles. The distribution in the right lead has a broad edge at $\epsilon=\mu-eV/2$ that corresponds to hot left-moving electrons. Due to interaction inside the wire this edge in region I sharpens.

In Fig. 4 we present the results for the distribution functions of left- and right-moving quasiparticles in the central (interacting) part of the wire [Eq. (43)]. For $K=0.2$ the plasmon reflection at the boundaries is strong. In a symmetric structure this leads to almost equal distribution functions of both types of carriers inside the wire.

In the upper panel of Fig. 5 we show the results for TDOS for $K=0.8$. The minima of TDOS are reached at energies $\epsilon=\mu\pm eV/2$. The broadening of the ZBA dips has two origins: smearing of the distribution function and dephasing. While the dephasing broadening [cf. second term in Eq. (38)] is the same for both chiral branches, the distribution functions [cf. first term in Eq. (38)] are in general different. A deeper minimum at $\epsilon=\mu+eV/2$ reflects the fact that right-moving electrons in the wire have a much narrower distribution function. This is because at $K=0.8$ the energy relaxation at the boundaries is quite weak, so that the distribution functions of cold right movers and hot left movers are only slightly modified. The situation is different for $K=0.2$ when distribution functions n_R and n_L are nearly identical (up to a shift by eV) (see Fig. 4). As a result, the structure of the TDOS also becomes symmetric. In fact, for the chosen value of the voltage, two broad ZBA dips merge together.

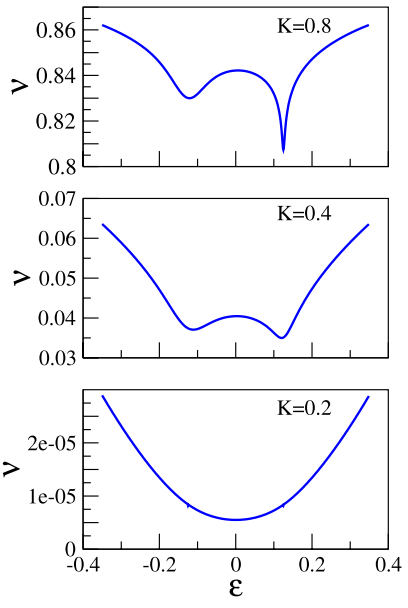

FIG. 5. (Color online) TDOS $\nu(\epsilon)$ (normalized to its noninteracting value $2\nu_0$) in the interacting region for $K=0.8$, 0.4, and 0.2. The temperatures of leads and the voltage are the same as in Fig. 3.

V. THERMAL CONDUCTIVITY AND ELECTRONIC DISTRIBUTION FUNCTION

We discuss now a relation between our results for the electron distribution function and previous findings on the electric and thermal conductance of a LL wire. In the absence of backscattering the number of left- and right-moving particles is separately preserved. As a result, the electric current is linear in the voltage V,

$$I = ev(N_R - N_L) = \frac{e^2}{h}V \tag{44}$$

with unrenormalized Landauer conductance $G=e^2/h$.[13–15,34] In our formalism, this relation immediately follows from Eq. (40) and the condition $\mathcal{F}_\eta(t\to 0)\to 0$. This ensures that the modification of the distribution function of right (or left) movers by a spatially varying interaction does not affect the integral of the distribution function over energy, i.e., the total number of carriers of each type.

We turn now to the thermal conductance. The energy current is easily found from the Green's functions of electrons in noninteracting parts of the wire,

$$I_E = v\partial_t[G_R^<(t,t') - G_L^<(t,t')]|_{t=t'}, \tag{45}$$

which can be rewritten in terms of the electron distribution functions,

$$I_E = \int_{-\infty}^{\infty} \frac{d\epsilon}{2\pi}\epsilon[n_L(\epsilon) - n_R(\epsilon)]. \tag{46}$$

Substituting results (40) and (39) for the distribution functions, we get the expression of the thermal current in terms of distribution functions of incoming electron-hole pairs,

$$I_E = \frac{1}{4\pi}\int_0^{\infty} d\omega\omega\mathcal{T}(\omega)[B_L^{(0)}(\omega) - B_R^{(0)}(\omega)]. \tag{47}$$

According to Eq. (47), the thermal conductance is affected by the interaction [through the reflection coefficient $\mathcal{T}(\omega)$], as was first found in Ref. 35. Note that due to the particle-hole symmetry of LL model, the applied voltage drops out of Eq. (47). For the case of sufficiently sharp boundaries, when $\mathcal{T}(\omega)$ can be considered as ω independent for relevant frequencies, Eq. (46) reduces to

$$I_E = \frac{\pi}{12}\mathcal{T}(T_R^2 - T_L^2). \tag{48}$$

Deviation of the transmission coefficient $\mathcal{T}(\omega)$ from unity leads to the violation of the Wiedemann-Franz law.[35] As is seen from our analysis, this deviation is a manifestation of a microscopic phenomenon: energy relaxation of electrons due to nonuniform interaction.

Heat current (47) can be equivalently represented in terms of plasmonic distributions in the wire,

$$I_E = \frac{1}{4\pi}\int_0^\infty d\omega\omega[B_L^{\mathrm{w}}(\omega) - B_R^{\mathrm{w}}(\omega)]. \tag{49}$$

This implies that the presentation of the heat current in form (46) is also valid in the interacting part of the wire, with the electronic distribution functions $n_\eta(\epsilon)$ given by Eq. (43). Thus, also in the interacting part of the wire, the energy current can be understood as carried by properly defined quasiparticle excitation. This is a remarkable result, which demonstrates that the concept of fermionic quasiparticles remains meaningful in a strongly interacting 1D system (LL) despite its non-Fermi-liquid features.

VI. SUMMARY AND OUTLOOK

To summarize, we have developed a theory of tunneling spectroscopy of LL conductor connected to reservoirs away from equilibrium. In the specific setup considered here, each branch originates from a source which is at equilibrium. However, the right and the left sources have different temperatures and different chemical potentials. We have modeled the system as a LL with spatially nonuniform interaction and calculated the single-electron Green's functions $G^{\gtrless}$ that carry information about the TDOS and the fermionic distribution functions in different parts of the wire. The interaction affects the tunneling characteristics in three distinct ways. First, it induces a power-law ZBA in the TDOS $\nu(\epsilon)$ (with two dips split by the voltage) in the interacting part of the wire. Second, it leads to broadening of ZBA singularities due to dephasing, with the dephasing rate governed by the interaction strength and the plasmon distribution inside the wire. Both the ZBA and the dephasing effects are encoded in the second term of Eq. (38).

The third effect of the interaction—which is specifically at the focus of the present work—is the inelastic scattering of electrons, leading to their redistribution over energies. This effect takes place in those regions where the interaction strength varies in space (near the wire boundaries in our model), inducing backscattering of plasmons (but not of electrons). This leads to relaxation of the electron distribution functions: left- and right-moving fermions "partly exchange" their distributions [see Eqs. (41) and (43) and Figs. 3–5]. For slowly varying interaction, when the plasmons with relevant frequencies go through essentially without reflection, the energy relaxation of electrons is negligible. In the opposite limit, when the plasmons are almost entirely reflected (due to strong and sharply switched interaction or, else, due to disordered boundary regions inducing the plasmon localization), the left and right movers essentially exchange their distribution functions (but not their total density). We have also discussed a connection between these results and earlier findings on the thermal conductivity of LL structures.

Our results are important for the analysis of TS experiments on strongly correlated 1D structures (in particular, carbon nanotubes[12]) out of equilibrium. In this connection, let us emphasize the following important point. What can actually be measured in experiment are Green functions, $G^>$ and $G^<$. The TDOS $\nu(\epsilon)$ in the interacting part of the wire, as well as the distribution function $n(\epsilon)$ in the noninteracting regions, is related to $G^>$ and $G^<$ in a simple way. On the other hand, in order to extract the distributions $n_R(\epsilon)$ and $n_L(\epsilon)$ from $G^{\gtrless}$ in the *interacting* part of the wire, a nontrivial deconvolution procedure is necessary. The broadening of (split) Fermi-edge structures in $G^{\gtrless}$ in the interacting part of the wire is governed by both the distribution function and the dephasing. The dephasing contributes to the smearing of Fermi-edge singularities also in higher-dimensional (diffusive) systems[36] and should be taken into account for the accurate interpretation of corresponding experiments.[11,37] In the 1D case the role of dephasing becomes particularly dramatic (if the interaction is sufficiently strong). This is very well illustrated by Fig. 5: two Fermi-edge singularities almost (middle panel) or even completely (lower panel) merge despite the fact that the Fermi edges in the distribution functions remain well separated (Fig. 4).

A comment of a more general nature is in order here. Our results illustrate the fact that there is no unique answer to the following question: "How much is a LL different from a Fermi liquid?" On one hand, the strong power-law ZBA in TDOS of a LL clearly distinguishes it from the Fermi liquid. In more formal terms, the single-particle residue Z, which is finite in the Fermi liquid, vanishes in a power-law fashion at the Fermi level of the LL. Also the dephasing rate determining the broadening of ZBA [Eq. (42)] is linear in temperature, contrary to the Fermi-liquid T^2 behavior. One could think that it makes little sense to speak about fermionic excitations in this situation, but this is not the case. First, the power-law vanishing of TDOS has little importance (like the value of Z in the Fermi liquid) for kinetic properties of the system. Second, dephasing rate (42) is governed by processes with zero energy transfer and do not lead to any energy relaxation. As a result, the distribution function of fermionic excitations, $n_\eta(\epsilon)$, is a fully meaningful concept even in the case of a strong interaction. It stays preserved as long as the interaction is spatially constant (or varies adiabatically slow with x). Furthermore, both the charge and the energy current in the interacting part of the wire can be understood as carried by these fermionic quasiparticles. From this point of view, the LL is a *perfect* Fermi liquid.

We conclude the paper by reviewing some future research prospects; the work in those directions is currently underway. First, one may consider a more general nonequilibrium situation where the distribution functions "injected" into the interacting part of the wire are of nonequilibrium (e.g., double-step) form by themselves[29,38] [see setups (b) and (c) in Fig. 1 in Ref. 29]; the first of these setups is close to the experimental situation in Ref. 12. This requires a generalization of

the bosonization technique that will be presented elsewhere.[33] Second, it is interesting to study correlations between outgoing left and right movers. In a general situation, one finds that their density matrices are not decoupled, i.e., they are entangled, which manifests itself, in particular, in current cross correlations. Third, one may study the effect of a random variation in the interaction strength $K(x)$ in the wire. If the wire is sufficiently long, plasmons with not too low frequencies get localized. Using our general results, one concludes that in the left (right) half of the wire both distributions n_R, n_L are determined by that of the left (respectively, right) reservoir, with a transition region which extends over the localization length of the middle section. To refine this picture, one has to include into consideration also plasmons with low frequencies (that remain delocalized). Also, including the spectral curvature will induce plasmon decay processes. (In the context of thermal conductivity, this physics was discussed in Ref. 35.) Finally, our results can be generalized to the case of chiral LL, where both branches move in the same direction, which is the situation characteristic for quantum-Hall edge-state devices.[10,39]

ACKNOWLEDGMENTS

We thank D. Bagrets, N. Birge, A. Finkelstein, I. Gornyi, D. Maslov, Y. Nazarov, D. Polyakov, and R. Thomale for useful discussions. We are particularly grateful to the late Yehoshua Levinson for numerous illuminating discussions on the physics of nonequilibrium systems. This work was supported by U.S.-Israel BSF, ISF of the Israel Academy of Sciences, Minerva Foundation, DFG under Grant No. SPP 1285 (Y.G.), EC Transnational Access Program at the WIS Braun Submicron Center (A.D.M.), German-Israeli Foundation under Grant No. 965, and Einstein Minerva Center.

APPENDIX A: MEASUREMENT OF THE GREEN'S FUNCTIONS $G^{\gtrless}$

The tunneling current between a probe and a quantum wire can be expressed in terms of the functions $G^{\gtrless}$ as

$$I(U) = \int dy dy' |T_{y,y'}|^2 \int \frac{d\epsilon}{\pi} [G^{<}_{\rm tp}(\epsilon - eU, y, y') G^{>}_{\rm w}(\epsilon, y', y) - G^{>}_{\rm tp}(\epsilon - eU, y, y') G^{<}_{\rm w}(\epsilon, y', y)], \quad \text{(A1)}$$

where the subscripts "tp" and "w" refer to the tunnel probe and the wire, respectively, U is a voltage between the tunneling probe and the wire, and $T(y,y')$ is a tunneling matrix element in the coordinate representation. If electron tunneling is local in space, we have $T(y,y')=T\delta(y-y')\delta(y-x)$, where x is a position of tunneling probe. Since the tunneling probe is at equilibrium, one can use a standard relation between the Green's functions and distribution function $n_{\rm tp}(\epsilon)$ of electrons in the probe,

$$G^{<}_{\rm tp}(\epsilon,x,x) = 2\pi i \nu_{\rm tp}(\epsilon) n_{\rm tp}(\epsilon),$$

$$G^{>}_{\rm tp}(\epsilon,x,x) = -2\pi i \nu_{\rm tp}(\epsilon)[1 - n_{\rm tp}(\epsilon)]. \quad \text{(A2)}$$

Differentiating the tunneling current with respect to voltage and substituting Eq. (A2) into Eq. (A1), one finds

$$\frac{\partial I}{\partial U} = -2i|T|^2 \int d\epsilon \left\{ \frac{\partial \nu_{\rm tp}(\epsilon - eU)}{\partial \epsilon} \{ n_{\rm tp}(\epsilon - eU) G^{>}_{\rm w}(\epsilon,x,x) + [1 - n_{\rm tp}(\epsilon - eU)] G^{<}_{\rm w}(\epsilon,x,x) \} - 2\pi i \nu_{\rm tp}(\epsilon - eU) \nu_{\rm w}(\epsilon) \frac{\partial n_{\rm tp}(\epsilon - eU)}{\partial \epsilon} \right\}. \quad \text{(A3)}$$

For a LL wire the Green's functions $G_{\rm w}$ and the TDOS $\nu_{\rm w}$ represent a sum of contributions of both chiral branches. If the density of states in the tunneling probe ($\nu_{\rm tb}$) is a constant (as in a normal metal), the first term in Eq. (A3) drops out. In this case the result is proportional to the TDOS in the wire. Assuming that the tunneling probe is at zero temperature, one then finds

$$\frac{\partial I}{\partial U} = 4\pi |T|^2 \nu_{\rm tp} \nu_{\rm w}(eU). \quad \text{(A4)}$$

On the other hand, if the density of states in the tunneling probe is strongly energy dependent (as for superconducting electrodes), the first term in Eq. (A3) survives. Unlike TDOS (which is determined by the difference $G^{>}_{\rm w} - G^{<}_{\rm w}$), this term contains also the information about $G^{>}_{\rm w} + G^{<}_{\rm w}$. Therefore, measurement of the tunneling current with two different types of tunneling probes (normal and superconducting) allows one to find functions $G^{>}_{\rm w}$ and $G^{<}_{\rm w}$ separately. The idea to use superconducting electrodes for the tunneling spectroscopy was introduced in Ref. 11 and more recently employed in Ref. 12.

APPENDIX B: THE GREEN'S FUNCTIONS $G^{\gtrless}$ AT THERMAL EQUILIBRIUM

At thermal equilibrium the Green's functions in the energy domain can be calculated explicitly. Using Eq. (38) and $B^{\rm w}_R = B^{\rm w}_L = B^0_R = B^0_L = \coth\frac{\omega}{2T}$, we find the exponent $\mathcal{F}_\eta(t)$ for the Green's functions in interacting part of the wire,

$$\mathcal{F}(t) = \gamma \ln \frac{\pi T}{i\Lambda \sinh \pi T(t - i/\Lambda)}, \quad \text{(B1)}$$

where we drop the chirality index η, as it is immaterial for $x=x'$ in equilibrium. Using Eq. (18) and performing a Fourier transform from the time into the energy domain, one finds

$$G^{>}(\epsilon) = -\frac{(\pi T)^{1+\gamma}}{2\pi v (i\Lambda)^\gamma} \int_{-\infty}^{\infty} dt e^{i\epsilon t} \frac{1}{\sinh^{1+\gamma} \pi T(t - i/\Lambda)}. \quad \text{(B2)}$$

After calculating an auxiliary integral, one obtains

$$\int_{-\infty}^{\infty} dt \frac{e^{izt}}{\sinh^{1+\gamma}(t - i0)} = \frac{i^{1+\gamma} 2^\gamma}{\Gamma(1+\gamma)} e^{\pi z/2} |\Gamma[(1 + \gamma + iz)/2]|^2,$$

$$G^{>}(\epsilon) = -\frac{i}{2\pi v}\frac{2^{\gamma}}{\Gamma(1+\gamma)}\left(\frac{\pi T}{\Lambda}\right)^{\gamma} e^{(\pi z/2)}|\Gamma[(1+\gamma+iz)/2]|^2, \tag{B3}$$

where $z=\epsilon/\pi T$. Similarly, one finds the function $G^{<}$,

$$G^{<}(\epsilon) = \frac{i}{2\pi v}\frac{2^{\gamma}}{\Gamma(1+\gamma)}\left(\frac{\pi T}{\Lambda}\right)^{\gamma} e^{-(\pi z/2)}|\Gamma[(1+\gamma+iz)/2]|^2. \tag{B4}$$

This yields the following asymptotic behavior of the Green's function at low temperatures ($|\epsilon| \gg T$),

$$G^{>}(\epsilon) = -\frac{i}{v\Gamma(1+\gamma)} e^{\pi(z-|z|)/2}\left(\frac{|\epsilon|}{\Lambda}\right)^{\gamma}, \tag{B5}$$

and high temperatures ($|\epsilon| \ll T$),

$$G^{>}(\epsilon) = -\frac{i}{2\pi v}\frac{2^{\gamma}}{\Gamma(1+\gamma)}\Gamma^2[(1+\gamma)/2]\left(\frac{\pi T}{\Lambda}\right)^{\gamma}. \tag{B6}$$

Using Eqs. (31), (B3), and (B4), one obtains TDOS at equilibrium,

$$\nu(\epsilon,T) = \frac{2^{\gamma-1}}{\pi^2 v\Gamma(1+\gamma)}\left(\frac{\pi T}{\Lambda}\right)^{\gamma}|\Gamma[(1+\gamma+iz)/2]|^2 \cosh\frac{\pi z}{2}. \tag{B7}$$

Equation (B7) describes the well-known ZBA in TDOS, $\nu(\epsilon) \propto |\epsilon|^{\gamma}$, smeared at the scale $\epsilon \sim 2\pi T(1+\gamma)$. This smearing results from a combined effect of (i) the thermal broadening of the distribution function and (ii) the dephasing rate[29] $1/\tau_{\phi}=2\pi\gamma T$.

It is straightforward to check that the Fermi-Dirac distribution function is recovered from the ratio

$$\frac{G^{>}(\epsilon)+G^{<}(\epsilon)}{G^{>}(\epsilon)-G^{<}(\epsilon)} = \tanh\frac{\epsilon}{2T} = 1-2n_0(\epsilon), \tag{B8}$$

in agreement with the fluctuation-dissipation theorem.

[1] M. Stone, *Bosonization* (World Scientific, Singapore, 1994).
[2] T. Giamarchi, *Quantum Physics in One Dimension* (Clarendon, Oxford, 2004).
[3] D. L. Maslov, in *Nanophysics: Coherence and Transport*, edited by H. Bouchiat, Y. Gefen, G. Montambaux, and J. Dalibard (Elsevier, New York, 2005), p. 1.
[4] J. von Delft and H. Schoeller, Ann. Phys. **7**, 225 (1998).
[5] M. Bockrath, D. H. Cobden, J. Lu, A. G. Rinzler, R. E. Smalley, L. Balents, and P. L. McEuen, Nature (London) **397**, 598 (1999); Z. Yao, H. W. Ch. Postma, L. Balents, and C. Dekker, *ibid.* **402**, 273 (1999).
[6] C. Schönenberger, Semicond. Sci. Technol. **21**, S1 (2006).
[7] O. M. Auslaender, A. Yacoby, R. de Picciotto, K. W. Baldwin, L. N. Pfeiffer, and K. W. West, Science **295**, 825 (2002); E. Levy, A. Tsukernik, M. Karpovski, A. Palevski, B. Dwir, E. Pelucchi, A. Rudra, E. Kapon, and Y. Oreg, Phys. Rev. Lett. **97**, 196802 (2006).
[8] E. Slot, M. A. Holst, H. S. J. van der Zant, and S. V. Zaitsev-Zotov, Phys. Rev. Lett. **93**, 176602 (2004); L. Venkataraman, Y. S. Hong, and P. Kim, *ibid.* **96**, 076601 (2006).
[9] A. N. Aleshin, H. J. Lee, Y. W. Park, and K. Akagi, Phys. Rev. Lett. **93**, 196601 (2004); A. N. Aleshin, Adv. Mater. **18**, 17 (2006).
[10] A. M. Chang, Rev. Mod. Phys. **75**, 1449 (2003); Y. Ji, Y. C. Chung, D. Sprinzak, M. Heiblum, D. Mahalu, and H. Shtrikman, Nature (London) **422**, 415 (2003) ; M. Dolev, M. Heiblum, V. Umansky, A. Stern, and D. Mahalu, *ibid.* **452**, 829 (2008); M. Grayson, L. Steinke, D. Schuh, M. Bichler, L. Hoeppel, J. Smet, K. v. Klitzing, D. K. Maude, and G. Abstreiter, Phys. Rev. B **76**, 201304(R) (2007).
[11] H. Pothier, S. Gueron, N. O. Birge, D. Esteve, and M. H. Devoret, Phys. Rev. Lett. **79**, 3490 (1997).
[12] Y. F. Chen, T. Dirks, G. Al-Zoubi, N. O. Birge, and N. Mason, Phys. Rev. Lett. **102**, 036804 (2009).
[13] D. L. Maslov and M. Stone, Phys. Rev. B **52**, R5539 (1995).
[14] V. V. Ponomarenko, Phys. Rev. B **52**, R8666 (1995).
[15] I. Safi and H. J. Schulz, Phys. Rev. B **52**, R17040 (1995); **59**, 3040 (1999).
[16] M. Khodas, M. Pustilnik, A. Kamenev, and L. I. Glazman, Phys. Rev. B **76**, 155402 (2007); A. M. Lunde, K. Flensberg, and L. I. Glazman, *ibid.* **75**, 245418 (2007).
[17] D. C. Mattis and E. H. Lieb, J. Math. Phys. **6**, 304 (1965).
[18] In fact, the word "relaxation" should be used with care in the present situation: as we show, emerging distribution functions are generically not of equilibrium (Fermi-Dirac) type.
[19] Y. Oreg and A. M. Finkelstein, Phys. Rev. Lett. **74**, 3668 (1995).
[20] J. Cao, Q. Wang, and H. Dai, Nature Mater. **4**, 745 (2005); V. V. Deshpande, B. Chandra, R. Caldwell, D. S. Novikov, J. Hone, and M. Bockrath, Science **323**, 106 (2009).
[21] W. Apel and T. M. Rice, Phys. Rev. B **26**, 7063 (1982).
[22] T. Giamarchi and H. J. Schulz, Phys. Rev. B **37**, 325 (1988).
[23] I. V. Gornyi, A. D. Mirlin, and D. G. Polyakov, Phys. Rev. Lett. **95**, 046404 (2005); Phys. Rev. B **75**, 085421 (2007).
[24] D. A. Bagrets, I. V. Gornyi, A. D. Mirlin, and D. G. Polyakov, Semiconductors **42**, 994 (2008).
[25] D. A. Bagrets, I. V. Gornyi, and D. G. Polyakov, arXiv:0809.3166 (unpublished).
[26] J. Rech and K. A. Matveev, Phys. Rev. Lett. **100**, 066407 (2008); J. Rech, T. Micklitz, and K. A. Matveev, *ibid.* **102**, 116402 (2009).
[27] H. C. Fogedby, J. Phys. C **9**, 3757 (1976); D. K. Lee and Y. Chen, J. Phys. A **21**, 4155 (1988); C. M. Naon, M. C. von Reichenbach, and M. L. Trobo, Nucl. Phys. B **435**, 567 (1995); C. M. Naon, M. J. Salvay, and M. L. Trobo, Int. J. Mod. Phys. A **19**, 4953 (2004); I. V. Yurkevich, in *Strongly Correlated Fermions and Bosons in Low-Dimensional Disordered Systems*, edited by I. V. Lerner, B. L. Altshuler, V. I. Falko, and T. Giamarchi (Kluwer, New York, 2002); A. Grishin, I. V. Yurkevich, and I. V.

Lerner, Phys. Rev. B **69**, 165108 (2004).

[28] I. V. Lerner and I. V. Yurkevich, in *Nanophysics: Coherence and Transport*, edited by H. Bouchiat, Y. Gefen, G. Montambaux, and J. Dalibard (Elsevier, New York, 2005), p. 109.

[29] D. B. Gutman, Y. Gefen, and A. D. Mirlin, Phys. Rev. Lett. **101**, 126802 (2008).

[30] For review of the Keldysh technique see, e.g., J. Rammer and H. Smith, Rev. Mod. Phys. **58**, 323 (1986); A. Kamenev, in *Nanophysics: Coherence and Transport*, edited by H. Bouchiat, Y. Gefen, G. Montambaux, and J. Dalibard (Elsevier, New York 2005), p. 177.

[31] Y. V. Nazarov, A. A. Odintsov, and D. A. Averin, Europhys. Lett. **37**, 213 (1997).

[32] In Ref. 29 we used notations $B^{v}_{\eta}(\omega)$ and $B^{u}_{\eta}(\omega)$ for these distribution functions.

[33] D. B. Gutman, Y. Gefen, and A. D. Mirlin, arXiv:0906.4076 (unpublished).

[34] Y. Oreg and A. M. Finkel'stein, Phys. Rev. B **54**, R14265 (1996).

[35] R. Fazio, F. W. J. Hekking, and D. E. Khmelnitskii, Phys. Rev. Lett. **80**, 5611 (1998); I. V. Krive, Low Temp. Phys. **24**, 377 (1998).

[36] D. B. Gutman, Y. Gefen, and A. D. Mirlin, Phys. Rev. Lett. **100**, 086801 (2008).

[37] A. Anthore, F. Pierre, H. Pothier, and D. Esteve, Phys. Rev. Lett. **90**, 076806 (2003).

[38] ZBA splitting in a similar setup was studied by S. G. Jakobs, V. Meden, and H. Schoeller, Phys. Rev. Lett. **99**, 150603 (2007).

[39] I. Neder, F. Marquardt, M. Heiblum, D. Mahalu, and V. Umansky, Nature Phys. **3**, 534 (2007); I. P. Levkivskyi and E. V. Sukhorukov, Phys. Rev. B **78**, 045322 (2008).